

Supplementary Information

Macroscopic crystalline deformation in an organic dye during reversible phase transition caused by alkyl disorder

Takaya Minami,^a Hiroyasu Sato^b and Shinya Matsumoto^{*a}

^a Graduate School of Environmental and Information Sciences, Yokohama National University, 79-7 Tokiwadai, Hodogaya-ku, Yokohama 240-8501, Japan.

E-mail: matsumoto-shinya-py@ynu.ac.jp

^b Rigaku Corporation, 3-9-12 Matsubara-cho, Akishima, Tokyo 196-8666, Japan.

E-mail: h-sato@rigaku.co.jp

Table of Contents

Experimental Procedures

1. General
2. Differential scanning calorimetry (DSC)
3. Single-crystal X-ray diffraction

Figures and tables

Scheme S1. Chemical structure of DE2.

Fig. S1 (a) Molecular arrangement of the crystal in the -A-B-B-A-B-B- pattern in the RT phase, (b) dihedral angles of the least squares planes of the conjugated system between molecules A (red) and B (green).

Fig. S2 Positions of the molecules viewing them from the (a) *a*, (b) *b*, and (c) *c* axes in the RT phase (molecules A and B are shown in red and green, respectively).

Fig. S3 Diffraction images from a DE2 single crystal during the phase transition, (a) measured at around 413 K, (b) at around 433 to 438 K, and (c) at around 453 K.

Fig. S4 Superposition of the packing diagram of the RT and HT phases; (a) viewing from the short molecular axis and (b) viewing from the long molecular axis (molecules A and B in the RT phase and molecules in the HT phase are shown in red, green, and purple, respectively).

Fig. S5 Centroid distances (a) between four molecules along the stacking direction and (b) along the short molecular axis in the RT and HT phases (molecules A and B in the RT phase and molecules in the HT phase are shown in red, green, and purple, respectively).

Fig. S6 Geometric parameters of the DE2 crystal in the RT phase; distances between molecular centroids (a) along the stacking direction and (b) along the short and long molecular axis (molecules A and B are shown in red and green, respectively).

Fig. S7 Isotropic temperature factors (U_{iso}) of the DE2 crystal correlated with selected carbon atoms from 143 to 393 K in the RT phase: the central ethylene carbon atoms (C2, C15, and C28), the phenyl ring carbon atoms (C5, C9, C18, C22, C31, and C35) and the carbon atoms of the terminal ethyl moieties (C11, C13, C24, C26, C37, and C39).

Table S1. Crystallographic data for DE2 in the LT, RT, and HT phases.

Table S2. Crystallographic data for the DE2 crystal from 143 to 393 K in the RT phase.

Table S3. Unit cell parameters of the RT phase from 143 to 393 K.

Movie S1. Microscope measurement of a plate crystal of DE2 upon heating (front view).

Movie S2. Microscope measurement of a plate crystal of DE2 upon cooling (front view).

Movie S3. Microscope measurement of a plate crystal of DE2 upon heating (side view).

Movie S4. Microscope measurement of a plate crystal of DE2 upon cooling (side view).

Movie S5. Microscope measurement of a prismatic crystal of DE2 upon heating and cooling.

Movie S6. Microscope measurement of another prismatic crystal of DE2 upon heating and cooling.

Movie S7. Microscope measurement of a plate crystal of DE2 upon heating and cooling with 8 x speed.

References

Experimental Procedures

1. General

All solvents were purchased from commercial sources and were used without further purification. DE2 was prepared according to a previously reported method and characterised by conventional spectroscopic methods.¹

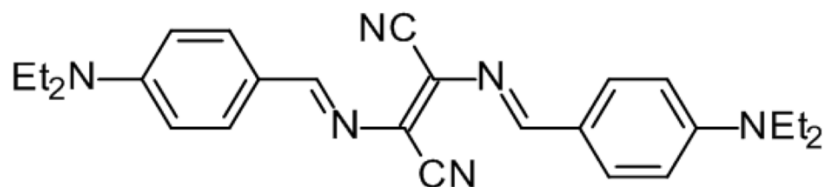
2. Differential scanning calorimetry (DSC)

DSC measurements were performed using a Rigaku Thermo plus DSC8230 at a heating and cooling rate of 20 K min⁻¹.

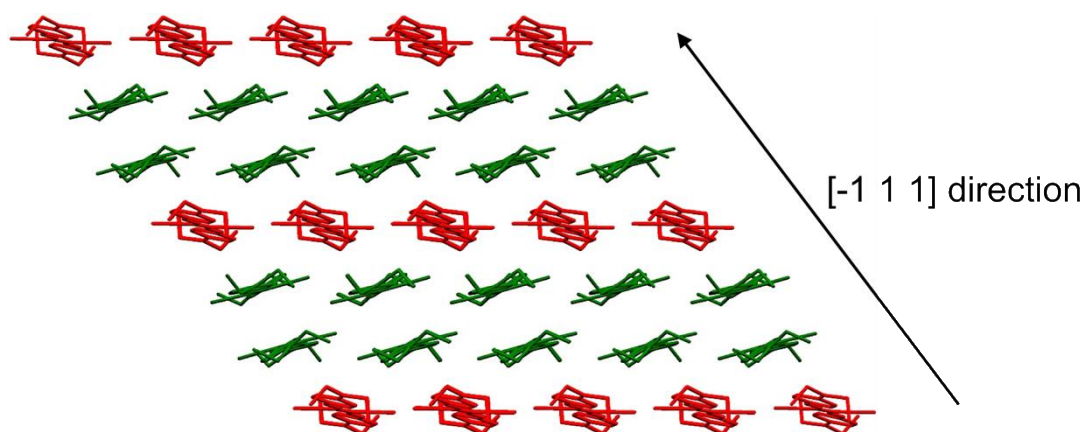
3. Single-crystal X-ray diffraction

The diffraction data for the single crystals of DE2 were collected at 443 K on a Rigaku XtaLAB P200 diffractometer using graphite-monochromated Mo $K\alpha$ radiation ($\lambda = 0.71075$ Å) and from 143 to 393 K on a Rigaku Mercury70 diffractometer using graphite-monochromated Mo $K\alpha$ radiation ($\lambda = 0.71075$ Å). Data reduction was performed using CrysAlisPro software.² The structures of DE2 were solved by direct methods using SHELXT and refined by full-matrix least-squares methods based on F^2 using SHELXL.^{3,4} All non-hydrogen atoms were anisotropically refined and the hydrogen atoms were refined with a riding model.

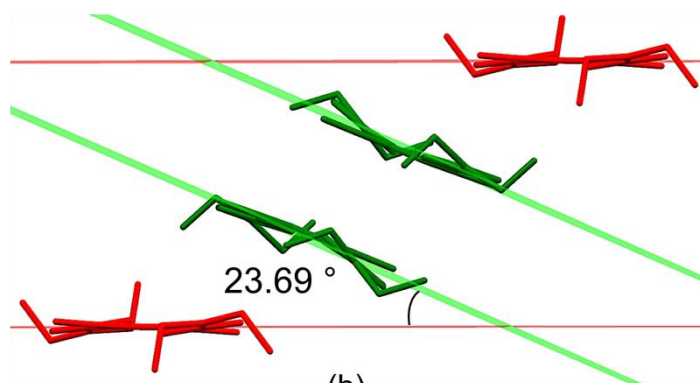
Figures and tables



Scheme S1. Chemical structure of DE2.



(a)



(b)

Fig. S1. (a) Molecular arrangement of the crystal in the -A-B-B-A-B-B- pattern in the RT phase, (b) dihedral angles of the least squares planes of the conjugated system between molecules A (red) and B (green).

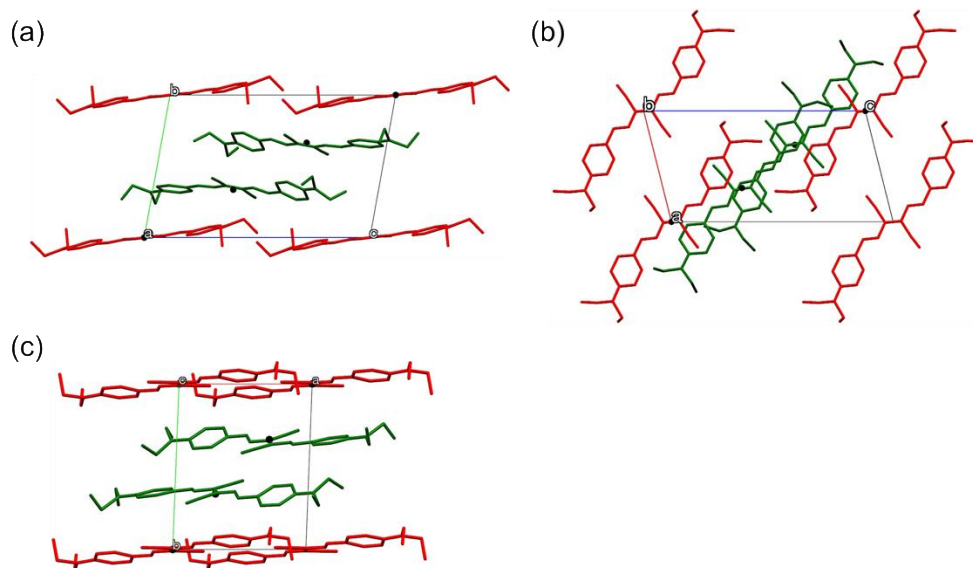


Fig. S2 Positions of the molecules viewing them from the (a) a , (b) b , and (c) c axes in the RT phase (molecules A and B are shown in red and green, respectively).

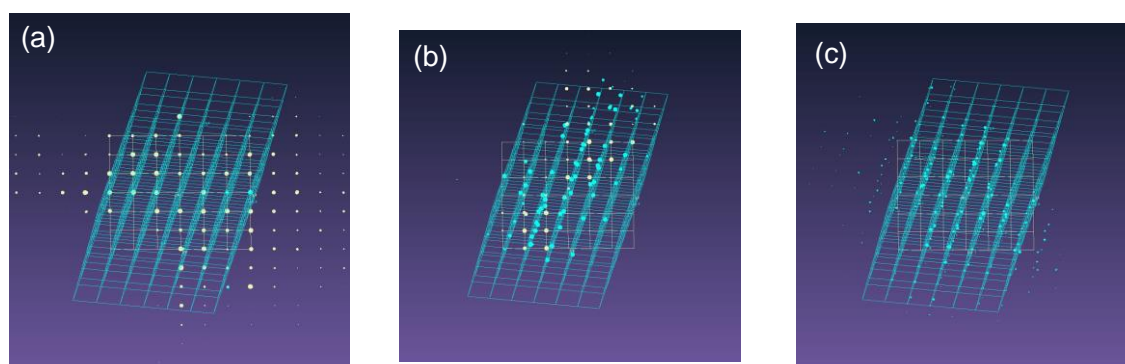


Fig. S3 Diffraction images from a DE2 single crystal during the phase transition, (a) measured at around 413 K, (b) at around 433 to 438 K, and (c) at around 453 K.

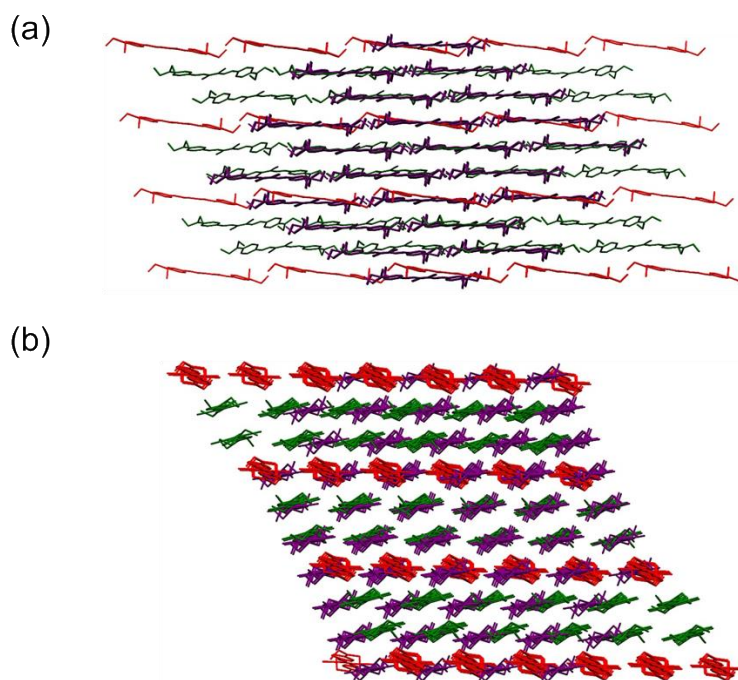


Fig. S4 Superposition of the packing diagram of the RT and HT phases; (a) viewing from the short molecular axis and (b) viewing from the long molecular axis (molecules A and B in the RT phase and molecules in the HT phase are shown in red, green, and purple, respectively).

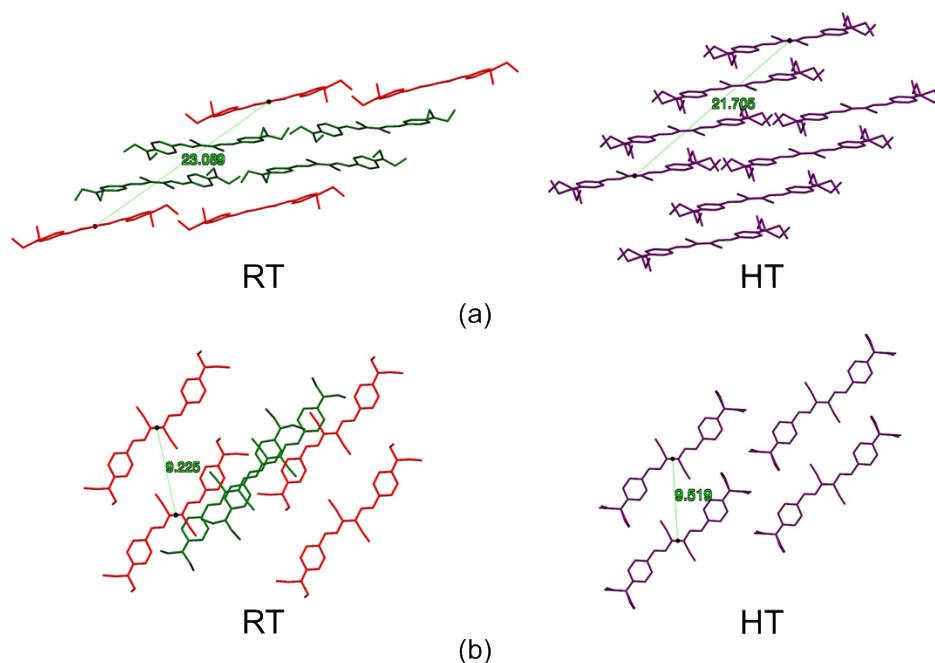


Fig. S5 Centroid distances (a) between four molecules along the stacking direction and (b) along the short molecular axis in the RT and HT phases (molecules A and B in the RT phase and molecules in the HT phase are shown in red, green, and purple, respectively).

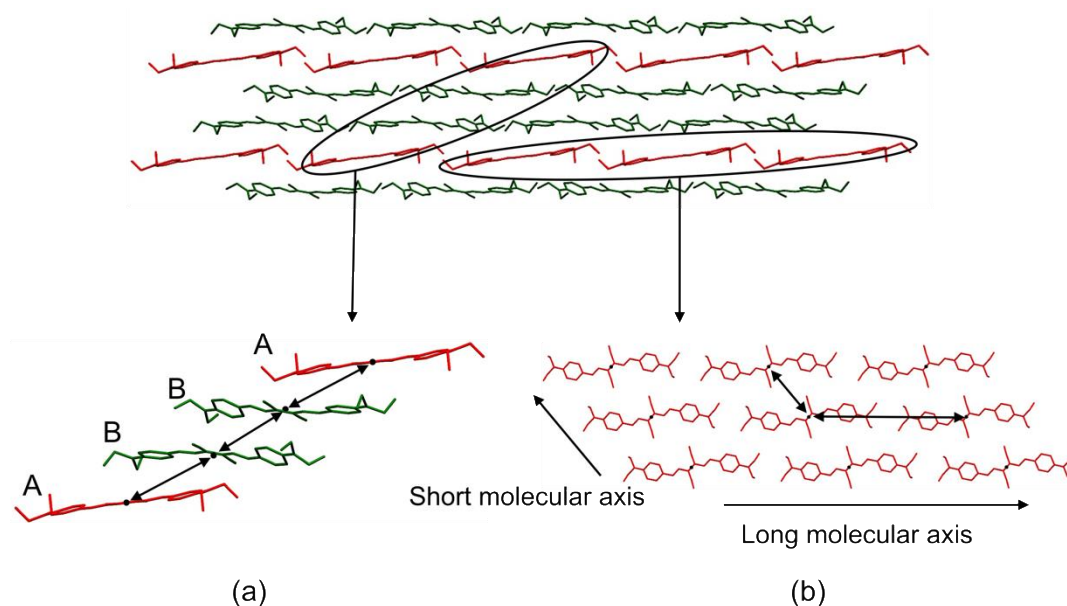


Fig. S6 Geometric parameters of the DE2 crystal in the RT phase; distances between molecular centroids (a) along the stacking direction and (b) along the short and long molecular axis (molecules A and B are shown in red and green, respectively).

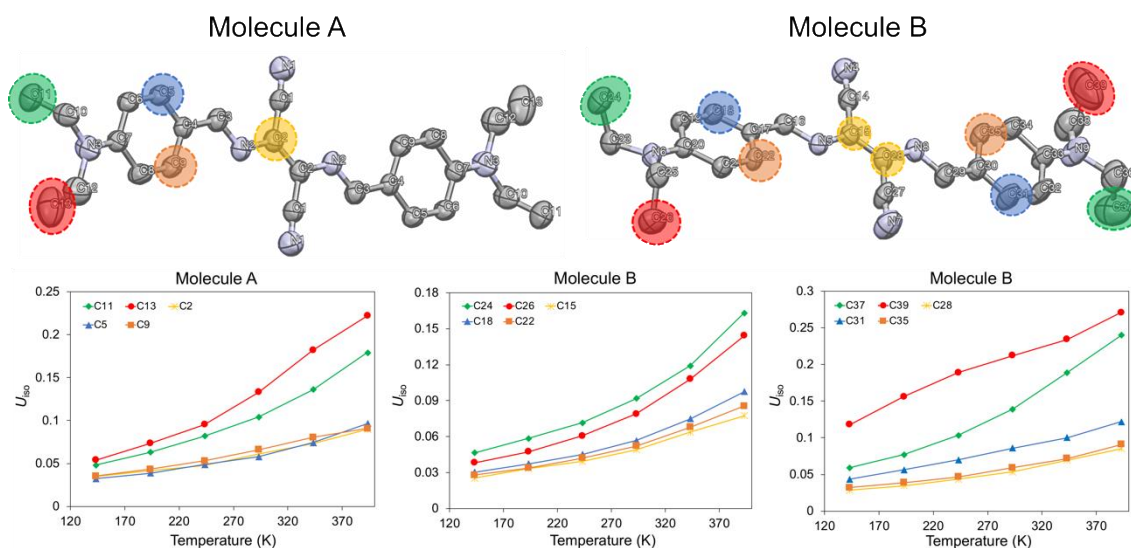


Fig. S7 Isotropic temperature factors (U_{iso}) of the DE2 crystal correlated with selected carbon atoms from 143 to 393 K in the RT phase: the central ethylene carbon atoms (C2, C15, and C28), the phenyl ring carbon atoms (C5, C9, C18, C22, C31, and C35) and the carbon atoms of the terminal ethyl moieties (C11, C13, C24, C26, C37, and C39).

Table S1. Crystallographic data for DE2 in the LT, RT, and HT phases.

	LT	RT	HT
Formula	$\text{C}_{26}\text{H}_{30}\text{N}_6$		
<i>F</i> _w	426.56		
Crystal size (mm)	$0.300 \times 0.200 \times 0.100$	$0.600 \times 0.120 \times 0.120$	$0.250 \times 0.094 \times 0.077$
Radiation	Mo <i>K</i> α	Cu <i>K</i> α	Mo <i>K</i> α
Wavelength (Å)	0.71075	1.5418	0.71075
Temperature (K)	93	298	443
Crystal system	Triclinic	Triclinic	Triclinic
Space group	<i>P</i> - 1	<i>P</i> - 1	<i>P</i> - 1
<i>a</i> (Å)	11.0395(5)	9.225(2)	7.2349(9)
<i>b</i> (Å)	18.0967(7)	11.290(3)	9.5192(15)
<i>c</i> (Å)	18.2548(7)	18.182(6)	9.8308(18)
α (°)	103.757(9)	79.94(3)	87.588(14)
β (°)	90.327(1)	76.09(2)	84.227(12)
γ (°)	100.315(1)	89.69(2)	70.714(13)
<i>V</i> (Å ³)	3480.6(2)	1808.5(8)	635.79(18)
<i>Z</i>	6	3	1
μ (mm ⁻¹)	0.075	0.563	0.068
<i>D</i> _{calc.} (g/cm ³)	1.221	1.175	1.114
Reflections collected	55975	6939	10243
Independent reflections	20060	6577	2358
(<i>R</i> _{int})	(<i>R</i> _{int} = 0.092)	(<i>R</i> _{int} = 0.019)	(<i>R</i> _{int} = 0.059)
<i>R</i> _I [<i>I</i> > 2σ(<i>I</i>)]	0.0596	0.0745	0.0758
<i>wR</i> ₂ (all data)	0.1378	0.1210	0.3135
Goodness-of-fit	0.817	1.530	0.965
CCDC No.	280142	280144	1811081

Table S2. Crystallographic data for the DE2 crystal from 143 to 393 K in the RT phase.

	143 K	193 K	243 K	293 K	343 K	393 K
Formula	$\text{C}_{26}\text{H}_{30}\text{N}_6$					
<i>F</i> _w	426.56					
Crystal size (mm)	0.481 × 0.154 × 0.104					
Radiation	Mo <i>K</i> α					
Wavelength (Å)	0.71075					
Crystal system	Triclinic	Triclinic	Triclinic	Triclinic	Triclinic	Triclinic
Space group	<i>P</i> - 1	<i>P</i> - 1	<i>P</i> - 1	<i>P</i> - 1	<i>P</i> - 1	<i>P</i> - 1
<i>a</i> (Å)	9.1533(4)	9.1682(4)	9.1764(4)	9.1906(5)	9.2410(5)	9.2864(7)
<i>b</i> (Å)	11.0888(4)	11.1406(4)	11.1823(4)	11.2290(6)	11.3265(6)	11.4128(7)
<i>c</i> (Å)	18.0746(7)	18.1008(7)	18.1079(7)	18.1200(9)	18.1906(10)	18.2356(12)
<i>α</i> (°)	100.192(3)	79.815(3)	79.869(3)	79.943(4)	80.038(5)	80.141(6)
<i>β</i> (°)	103.814(4)	76.166(4)	76.150(3)	76.137(4)	76.141(5)	76.139(6)
<i>γ</i> (°)	90.080(3)	89.991(3)	89.880(3)	89.745(4)	89.607(5)	89.451(6)
<i>V</i> (Å ³)	1751.55(13)	1765.17(13)	1774.40(12)	1786.27(17)	1819.49(18)	1847.7(2)
<i>Z</i>	3	3	3	3	3	3
<i>μ</i> (mm ⁻¹)	0.075	0.074	0.074	0.073	0.072	0.071
<i>D</i> _{calc.} (g/cm ³)	1.213	1.204	1.197	1.190	1.168	1.150
Reflections collected	11335	11451	11551	11413	11703	11805
Independent reflections	6055	6120	6158	6050	6186	6260
<i>R</i> _{int}	0.0324	0.0345	0.0353	0.0388	0.0392	0.0448
<i>R</i> _I [<i>I</i> > 2σ(<i>I</i>)]	0.0684	0.0719	0.0783	0.0818	0.0841	0.0857
<i>wR</i> ₂ (all data)	0.1855	0.1991	0.2265	0.2478	0.2665	0.2965
Goodness-of-fit	1.026	1.020	1.026	1.026	1.020	0.956
CCDC No.	1811066	1811070	1811069	1811067	1811071	1811068

Table S3. Unit cell parameters of the RT phase from 143 to 393 K.

	143 (K)	$\Delta^{[a]}$ (%)	193 (K)	$\Delta^{[a]}$ (%)	243 (K)	$\Delta^{[a]}$ (%)	293 (K)	$\Delta^{[a]}$ (%)	343 (K)	$\Delta^{[a]}$ (%)	393 (K)
<i>a</i> (Å)	9.153	0.16	9.168	0.09	9.176	0.15	9.191	0.55	9.241	0.49	9.286
<i>b</i> (Å)	11.089	0.47	11.141	0.37	11.182	0.42	11.229	0.87	11.327	0.76	11.413
<i>c</i> (Å)	18.075	0.14	18.101	0.04	18.108	0.07	18.120	0.39	18.191	0.25	18.236

[a] This value indicates the rate of change of the cell parameters between two temperature regions.

References

- 1 K. Shirai, M. Matsuoka, K. Fukunishi, *Dyes Pigm.*, 2000, **47**, 107.
- 2 CrysAlisPro: Data Collection and Processing Software, Rigaku Corporation (2015). Tokyo 196-8666, Japan.
- 3 SHELXT Version 2014/5: Sheldrick, G. M. (2014). *Acta Cryst.* A70, C1437.
- 4 SHELXL Version 2014/7: Sheldrick, G. M. (2008). *Acta Cryst.* A64, 112-122.